ISSN 1936-878X/08/$34.00
PUBLISHED BY ELSEVIER INC.
DOI:10.1016/j.jcmg.2008.06.001

Detection of Lipid Core Coronary Plaques in Autopsy Specimens With a Novel Catheter-Based Near-Infrared Spectroscopy System

Craig M. Gardner, PhD,* Huwei Tan, PhD,* Edward L. Hull, PhD,*
Jennifer B. Lisauskas, MS,* Stephen T. Sum, PhD,* Thomas M. Meese, BS,*
Chunsheng Jiang, PhD,* Sean P. Madden, PhD,* Jay D. Caplan, BS, MBA,*
Allen P. Burke, MD,† Renu Virmani, MD,‡ James Goldstein, MD,§ James E. Muller, MD*
Burlington, Massachusetts; Washington, DC; Gaithersburg, Maryland; and Royal Oak, Michigan

OBJECTIVES This study sought to assess agreement between an intravascular near-infrared spectroscopy (NIRS) system and histology in coronary autopsy specimens.

BACKGROUND Lipid core plaques cannot be detected by conventional tests, yet are suspected to be the cause of most acute coronary syndromes. Near-infrared spectroscopy is widely used to determine the chemical content of substances. A NIRS system has been developed and used successfully in 99 patients.

METHODS Scanning NIRS was performed through blood in 212 coronary segments from 84 autopsy hearts. One histologic section was analyzed for every 2 mm of artery. Lipid core plaque of interest (LCP) was defined as a lipid core >60° in circumferential extent, >200-μm thick, with a mean fibrous cap thickness <450 μm. The first 33 hearts were used to develop the algorithm; the subsequent 51 validation hearts were used in a prospective, double-blind manner to evaluate the accuracy of NIRS in detecting LCP. A NIRS-derived lipid core burden index for an entire artery was also validated by comparison to histologic findings.

RESULTS The LCPs were present in 115 of 2,649 (4.3%) sections from the 51 validation hearts. The algorithm prospectively identified LCP with a receiver-operator characteristic area of 0.80 (95% confidence interval [CI]: 0.76 to 0.85). The lipid core burden index detected the presence or absence of any fibroatheroma with an area under the curve of 0.86 (95% CI: 0.81 to 0.91). A retrospective analysis of lipid core burden index conducted in extreme artery segments with either no or extensive fibroatheroma yielded an area under the curve of 0.96 (95% CI: 0.92 to 1.00), confirming the accuracy of spectroscopy in identifying plaques with markedly different lipid content under ideal circumstances.

CONCLUSIONS This novel catheter-based NIRS system accurately identified lipid core plaques through blood in a prospective study in coronary autopsy specimens. It is expected that this novel capability will be of assistance in the management of patients with coronary artery disease. (J Am Coll Cardiol Img 2008;1:638–48) © 2008 by the American College of Cardiology Foundation

From *InfraReDx, Inc., Burlington, Massachusetts; †Division of Cardiovascular Pathology, Armed Forces Institute of Pathology, Washington, DC; ‡CVPath Institute, Gaithersburg, Maryland; and the §Division of Cardiology, William Beaumont Hospital, Royal Oak, Michigan. InfraReDx was the sole source of financing for this study. Drs. Gardner, Tan, Hull, Sum, Jiang, Madden, and Muller, and Ms. Lisauskas, Mr. Meese, and Mr. Caplan are current employees of InfraReDx or were employees at the time of this study. Dr. Goldstein is an InfraReDx consultant and equity owner. Drs. Burke and Virmani were consultants to InfraReDx for histologic studies.

Manuscript received March 18, 2008; revised manuscript received May 12, 2008, accepted June 10, 2008.

Extensive evidence suggests that coronary artery plaques with a lipid core are the cause of most acute coronary events (1,2). Unfortunately, current diagnostic techniques, including invasive coronary angiography, cannot identify these presumably high-risk structures. Although near-infrared spectroscopy (NIRS) is widely used in many disciplines to identify the chemical composition of unknown substances, including lipids, it has not been possible to use this powerful analytic technique to examine the composition of coronary plaques in living patients.

See page 649

Over the past decade, studies conducted by multiple groups have documented that NIRS can accurately identify lipid-rich atherosclerotic plaques in autopsy specimens under laboratory conditions (3). None of these ex vivo studies has addressed the full range of difficulties that would be encountered in examination of coronary plaques in patients. To perform spectroscopic assessment of coronary plaques, the NIRS device would need to access the artery, use wavelengths that can penetrate blood, scan the length and circumference of the artery, and obtain measurements at sufficient speed to overcome interference due to cardiac motion. A catheter-based spectroscopy system that fulfills these 4 criteria has been developed and used successfully to obtain NIRS measurements in 99 patients (4).

The purpose of the present study was to test the ability of this NIRS system to detect lipid core plaques in human coronary artery autopsy specimens in which the gold standard of histology is available. The system consists of a near-infrared laser, an optical catheter similar in size and use to an intravascular ultrasound catheter, a pullback and rotation device, and an analytic algorithm to calculate the probability that a lipid core plaque is present at each location examined. The algorithm was developed with the use of a calibration set of 86 human coronary artery segments from 33 hearts and then tested in a prospective study of 126 coronary segments from 51 hearts. The NIRS measurements were obtained under pressure, temperature, and blood flow conditions simulating those encountered in patients undergoing catheterization.

METHODS

The NIRS calibration and validation measurements were obtained over 2 years in specimens from 84 human hearts. The last 51 hearts were used in the validation study with a finalized NIRS algorithm and prospectively defined end points. The analysis was double-blinded: those constructing the algorithm in the calibration phase did not have access to histologic data from the validation phase, and those performing the NIRS and histologic analyses during the validation phase did not have access to the algorithm.

Specimens. Hearts were acquired from the National Disease Research Interchange or the International Institute for the Advancement of Medicine per a protocol approved by an institutional review board. Hearts were received within 48 h after death, maintained on ice at 4°C and measured within 96 h after death. The major coronary arteries were examined in situ using angioscopy to exclude severely stenotic or occluded segments impassable (<1 mm diameter) by the NIRS catheter.

Following angioscopic screening, arterial segments with epivascular tissue were harvested for measurement. Side branches were ligated to prevent loss of blood during perfusion. Each arterial segment was then mounted in a custom fixture (Fig. 1A) and both ends of the segment were attached to luer connectors that allowed fluid flow and catheter entry.

NIRS. The 3.2-F InfraReDx (Burlington, Massachusetts) NIRS catheter (Fig. 1D) was advanced along a 0.014-inch guidewire through the segment mounted in the fixture. The segment was perfused with human blood at body temperature. A varistaltic pump (Manostat, Barnant Corp., Barrington, Illinios) supplied pulsatile blood flow at 60 cycles/min, providing a flow rate of approximately 130 ml/min. Outflow pressure was maintained at 80 to 120 mm Hg. Spectral data were collected inside the segment during automated NIRS catheter pullback at 0.5 mm/s and 240 rpm.

Histopathology. After the NIRS measurements were obtained, the segments were pressure-fixed in formalin and decalcified with EDTA. Each segment was then cut perpendicular to the longitudinal axis of the vessel at 2-mm intervals of the fixture's guideposts (Fig. 1B). Two 5-μm histopathology slides were prepared at the CVPath Institute from the distal side of each 2-mm block and stained with hematoxylin-eosin and Russell-Movat's pentachrome, respectively. Histologic features of the arteries were classified by a CVPath pathologist (A.P.B.) according to a modified American Heart Association classification scheme (5).

ABBREVIATIONS AND ACRONYMS

AUC = area under the curve
IVUS = intravascular ultrasound
LCBI = lipid core burden index
LCP = lipid core plaque of interest
NIRS = near-infrared spectroscopy
ROC = receiver-operator characteristic

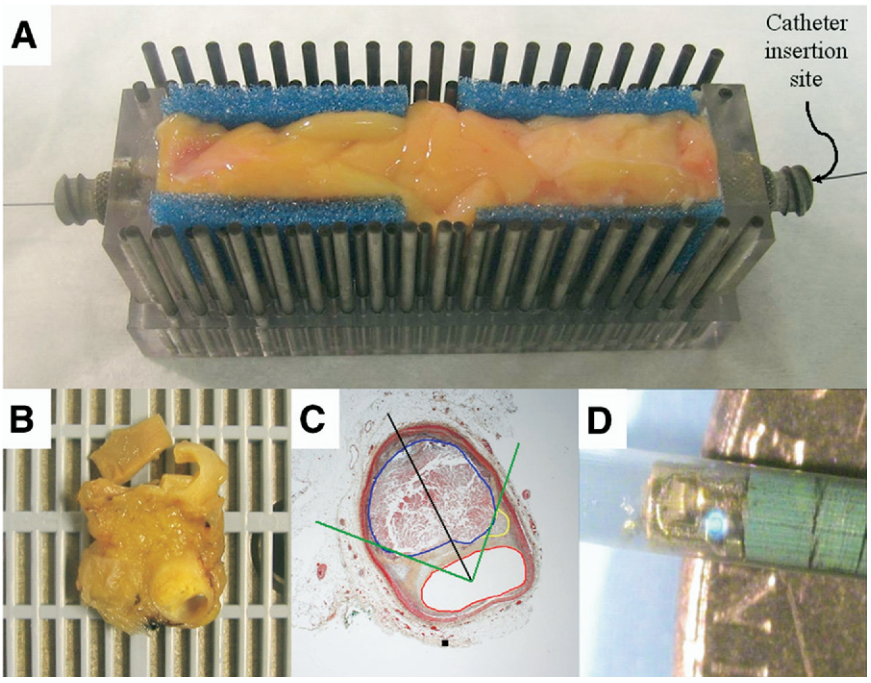

Figure 1. Apparatus for Fixing an Arterial Sample, Gross and Histologic Views, and Close-Up of NIRS Catheter

(A) A coronary artery segment mounted in a fixture to ensure registration of intraluminal near-infrared spectroscopy (NIRS) signals with histology. The vertical rods permit precise sectioning at 2-mm intervals. **(B and C)** Gross and microscopic cross-sections. Histomorphometry outlines show the lumen **(red)**, lipid core **(blue)**, and a small lipid pool **(yellow)**. The angle subtended by the lipid core is shown in **green**. Radii used to measure cap and core thickness are in **black. (D)** The imaging tip of the NIRS catheter lying on a U.S. penny.

Each histopathology slide was digitized using a standard microscope at 1.25× magnification. Using custom software, contours were drawn on each image to identify fiducial markers retained by the tissue-preparation inking scheme, the lumen boundary, lipid pools at sites of pathological intimal thickening, and noncalcified and calcified lipid cores in fibroatheroma (Fig. 1C).

To provide a quantitative target suitable for algorithm construction and validation, a lipid core plaque of interest (LCP) was defined as fibroatheroma with lipid core >60° in circumferential extent, >200 μm thick, with a fibrous cap having a mean thickness <450 μm. Using this definition, each block that was of adequate quality for histologic classification and histomorphometry was classified as either positive or negative for presence of LCP. Also, the normalized lipid core volume was defined as the total lipid core volume identified by histomorphometry in a segment divided by the segment length and was used to assess accuracy of NIRS at the segment level.

Correlation between NIRS and histopathology. Both algorithm calibration and validation require longitudinal coregistration of NIRS data with the histology truth standard. To accomplish this, the pullback location of the distal metal luer's inner edge was identified in a NIRS pullback, labeled as the 0-mm pullback position, and associated with the distal-most histology thin section.

The outputs of the NIRS algorithm for each pullback, which will be described in Figure 3, are a chemogram image, a block chemogram, and a lipid core burden index (LCBI). The ability of NIRS to detect localized LCP in 2-mm blocks was evaluated using receiver-operator characteristic (ROC) analysis of the NIRS block chemogram intensity values versus the LCP truth values from histology for all 2-mm blocks with lumen diameters ≤3 mm. The ability of NIRS to detect the presence of any-sized fibroatheroma in an artery segment was evaluated using ROC analysis of the LCBI values versus histology truth (presence or absence of fibroatheroma).

Statistics. The study was powered to test the null hypothesis that the area under the curve (AUC) for detecting LCP in lumens ≤3 mm in diameter would be ≤0.72. The required sample size was estimated for 80% power and 95% confidence interval (CI) (2-sided) using the power calculations

appropriate for AUC testing (6) using PASS statistical software (NCSS, Kaysville, Utah).

Statistical analyses were performed using MATLAB (The MathWorks, Inc., Natick, Massachusetts). Confidence intervals were 2-sided 95% levels and were calculated using a bootstrap method that accounts for the possibility of any within-segment and within-heart correlations (7). All donor and LCP characteristics were not normally distributed and therefore are reported as median with interquartile range for non-normal data.

RESULTS

Donor and tissue characteristics. Table 1 shows the characteristics for the 51 validation hearts. The perfusate blood lipid chemistry covered a wide range of profiles and was not correlated with hematocrit (data not shown). Histopathologic examination of each 2-mm segment identified 115 LCP (4.3%) in 30 of 51 donors (59%), the characteristics of which are presented in Table 2.

Yield of adequate data. A total of 2,496 blocks from 126 segments and 51 hearts were histologically and spectrally adequate for the validation phase (Fig. 2). In addition to block adequacy, analysis of the LCBI required assessment of each segment's data adequacy. Five segments were excluded because >25% of the chemogram pixels were spectrally inadequate, and 1 was excluded because 8 of its 26 blocks were not processed or were histologically inadequate.

Table 1. Clinical Characteristics of Heart Donors in Validation Data Set at Time of Death

Characteristic	Value
Number	51
Demographic profile	
Male, n (%)	36 (71)
Age in yrs, median (interquartile range)	68 (53–81)
Medical history, n (%)	
Hypertension	31 (61)
Chronic smoker	21 (41)
Diabetes mellitus	17 (33)
Prior presentation CHF	16 (31)
Prior MI	11 (22)
Prior CABG	4 (8)
Cause of death, n (%)	
Cardiovascular related	40 (78)
Cerebrovascular accident	15 (29)
Cardiac arrest	13 (25)
MI	7 (14)
Cardiopulmonary arrest	3 (6)
Other cardiac cause	2 (4)
Noncardiovascular related	8 (16)
Unknown	3 (6)

Complete characteristics were not available for all donors.
CABG = coronary artery bypass graft; CHF = congestive heart failure; MI = myocardial infarction.

Table 2. Characteristics of LCPs in Validation Data Set

Characteristic	Value
n (%)	115 (4.3)
Number per heart, n (interquartile range)	1 (0–4)
Number contained in artery, n (%)	
Left anterior descending	47 (41)
Left circumflex	25 (22)
Right	43 (37)
Distance from ostium (mm)	
Left anterior descending	32 (23–42)
Left circumflex	18 (12–39)
Right	60 (27–84)
Lumen diameter (mm)	2.4 (2.0–2.9)
Number with calcified core, n (%)	45 (39)
Cross-sectional area (mm^2)	1.2 (0.8–2.1)
Minimum cap thickness (μm)	164 (101–243)
Core thickness (μm)	448 (315–565)
Plaque angle (°)	102 (77–132)

All continuous variables reported as median (interquartile range).
LCP = lipid core plaque of interest.

Validation. Outputs of the NIRS algorithm (chemogram and block chemogram) for a segment containing LCP and for a normal segment are shown in Figures 3 and 4. The primary analysis was conducted by comparing the block chemogram readings with histologic classifications using all 1,909 adequate 2-mm blocks with lumen diameters ≤ 3 mm. The ROC analysis resulted in an AUC of 0.80 (95% CI: 0.76 to 0.85) (Fig. 5). Exploratory analyses that assess the accuracy of extreme cases for which there are fewer sources of false-positives and false-negatives are also presented in Figure 5. The AUCs in these exploratory analyses were 0.89 (95% CI: 0.85 to 0.94) and 0.87 (95% CI: 0.77 to 0.97). Sources of false-positive and false-negative readings are shown in Figure 6.

The LCBI values for 120 segments from 51 hearts were exponentially distributed (range: 0 to 322) and are plotted against categorized normalized lipid core volume in Figure 7. The ROC curve for NIRS detecting an artery with lipid core is shown in Figure 8 and resulted in an AUC of 0.86 (95% CI: 0.81 to 0.91). Also shown in the figure is an ROC curve for an exploratory analysis for detecting clinically high lipid core burden using the LCBI, which resulted in an AUC of 0.96 (95% CI: 0.92 to 1.00).

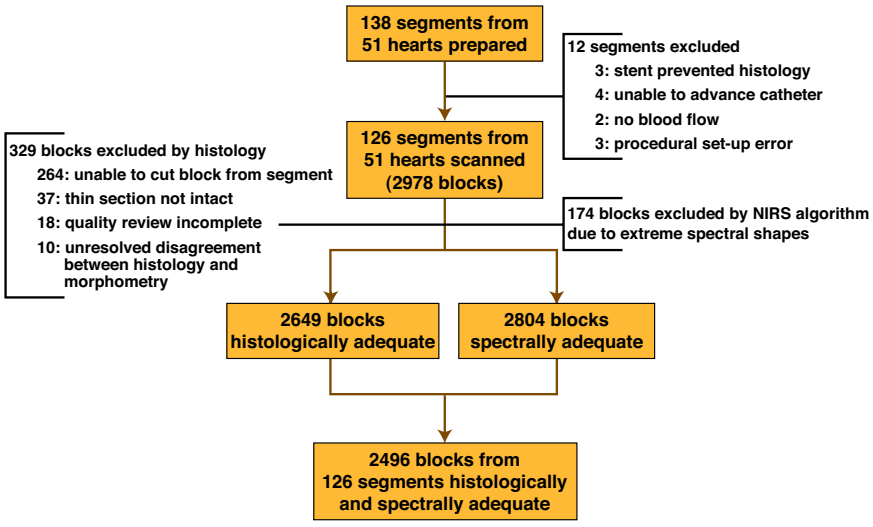

Figure 2. Flow Chart of Inclusion Criteria

Flow diagram describing the selection of data that met prospectively specified histologic and spectral criteria for inclusion in the blinded validation. NIRS = near-infrared spectroscopy.

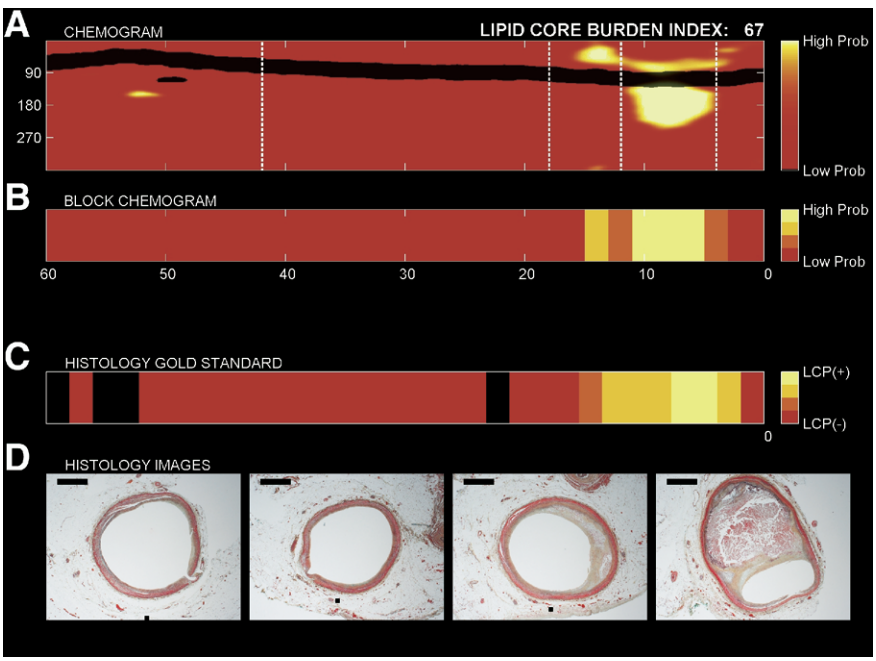

Figure 3. A NIRS Scan Correlates Well to Histologic Findings in Coronary Artery From an 85-Year-Old Male With a History of MI

(A) Chemogram image indicating artery wall lipid content (x axis = pullback in millimeters; y axis = rotation in degrees). Each pixel is marked with **red** for low probability and **yellow** for high probability of lipid core plaque of interest (LCP). The lipid core burden index **(top right)** indicates amount of lipid in scanned artery on a 0 to 1,000 scale. **(B)** Summary (block chemogram) of LCP presence at 2-mm intervals in 4 probability categories. **(C)** Map of histologic classifications (**yellow** = LCP; **light orange** = small or thick-capped fibroatheroma; **dark orange** = intimal xanthoma and pathologic intimal thickening; **red** = all other types). **(D)** Movat cross-sections from locations along the artery **(dotted lines). Black bars** denote 1 mm. Image interpretation: The chemogram shows prominent lipid core signal at 2 to 16 mm, occupying 180°. The block chemogram shows that the strongest LCP signals extend 5 to 11 mm. The NIRS signals at 18 and 42 mm correctly indicate absence of LCP. MI = myocardial infarction; other abbreviations as in Figure 1.

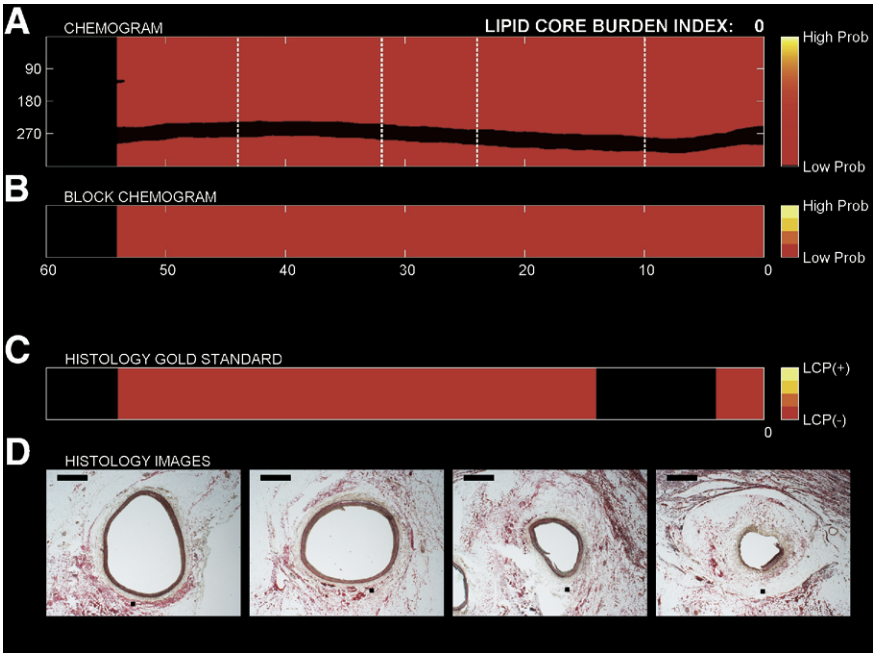

Figure 4. A Chemogram From a 45-Year-Old Female Who Died of Anoxia

The NIRS reading of no LCP is confirmed by histology. Abbreviations as in Figures 1 and 3.

DISCUSSION

This study demonstrates that this novel catheter-based NIRS system can identify lipid core plaques through blood in human coronary artery autopsy specimens as validated by histology. The AUC values obtained for detection of localized LCPs and of any fibroatheroma were 0.80 and 0.86, respectively. These values are representative of the performance of commonly used intravascular and other diagnostic modalities (8–10).

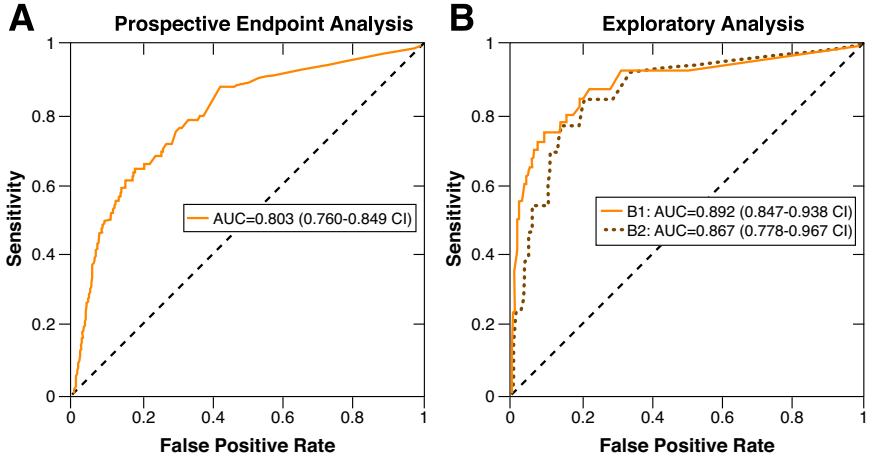

Figure 5. ROC Curves Showing Agreement Between NIRS Signals (as Indicated by Block Chemogram) and Histology

(A) Prespecified end point analysis to discriminate 2-mm blocks containing LCP from blocks containing all other tissue types in blocks with lumen diameters ≤3 mm. **(B)** Exploratory analyses conducted in blocks with lumen diameters ≤2.5 mm. **(B1)** Discrimination of blocks containing noncalcified LCPs versus blocks without lipid. **(B2)** Discrimination of LCPs identified by requiring block chemograms that span 3 or more consecutive 2-mm blocks from all other tissue types. AUC = area under the curve; ROC = receiver-operator characteristic; other abbreviations as in Figures 1 and 3.

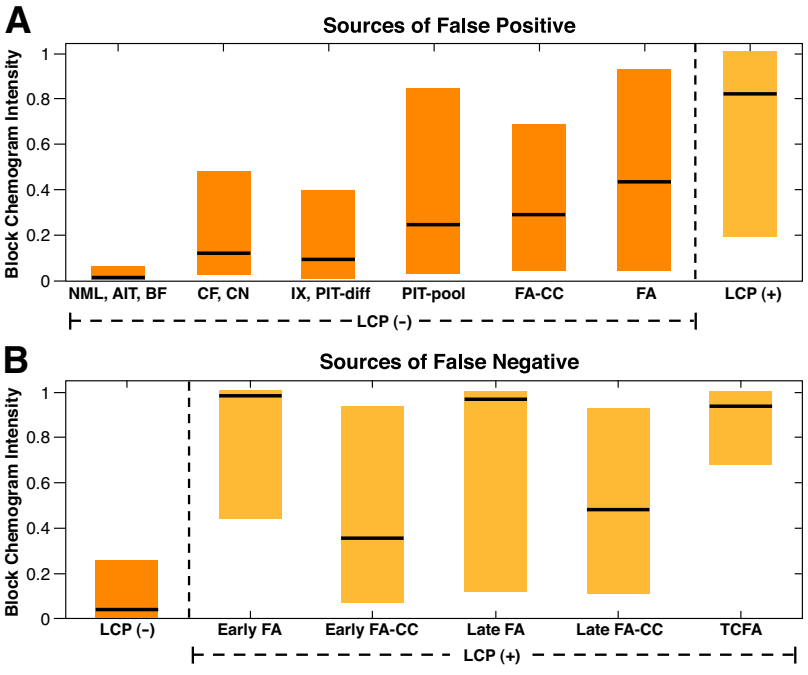

Figure 6. Sources of False Positive and False Negative

The graph displays medians **(horizontal lines)** and interquartile ranges **(boxes)** of block chemogram readings for different histologic classifications. **(A)** The LCP-negative class expanded into histologic subtypes. Higher y-axis values for LCP-negative result in false-positive readings. Fibroatheroma that were too small or thick-capped to be defined as LCP (FA) were the major source of false-positive readings. **(B)** The LCP-positive class expanded into histologic subtypes. Lower y-axis values for LCP-positive result in false-negative readings. The LCPs with calcified cores (Early FA-CC and Late FA-CC) were the main source of false-negative readings. AIT = adaptive intimal thickening; BF = bland fibrous plaque; CF = calcified fibrous plaque; CN = calcified nodule; -diff = spatially diffuse lipid; FA = fibroatheroma without calcified core; FA-CC = fibroatheroma with calcified necrotic core; IX = intimal xanthoma; NML = normal tissue; PIT = pathologic intimal thickening; -pool = spatially localized lipid pools; TCFA =thin-capped fibroatheroma; other abbreviations as in Figure 3.

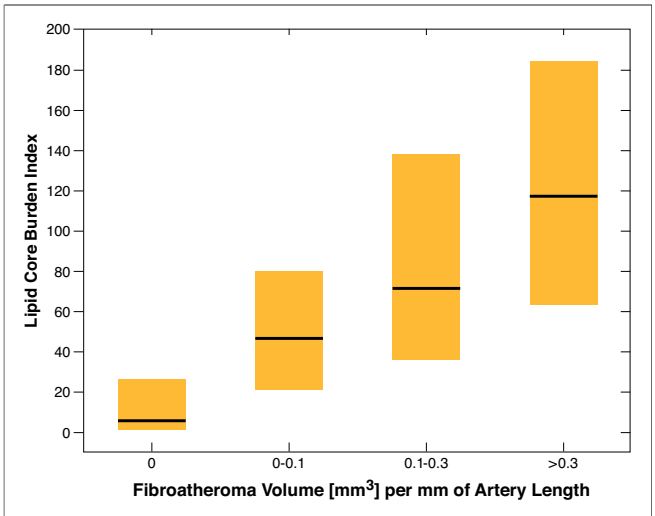

Figure 7. LCBI Values for Normalized Lipid Core Volume per Artery Segment

Medians **(horizontal lines)** and interquartile ranges **(boxes)** of lipid core burden index (LCBI) values for no, low, intermediate, and high ranges of normalized lipid core volume per artery segment based on histologic findings.

Using a threshold separating the 2 middle colors in the block chemograms of Figures 3 and 4, the sensitivity, specificity, positive predictive value, and negative predictive value were 49%, 90%, 19%, and 97%, respectively, in detecting localized LCP. The low positive predictive value was expected due to its strong dependence on disease prevalence, which was 4% in this study. The prevalence of LCP in ruptured plaques is approximately 70% (1), which would result in positive and negative predictive values of 92% and 43%, respectively, if the same sensitivity and specificity were achieved in the subset of artery wall-containing ruptured plaques.

The present study is similar to ex vivo validation studies of other intracoronary imaging devices (11–14) in that we measured fresh coronary artery tissue at body temperature from multiple donors and compared it with the histology. Our study differs in that we perfused the arteries with blood rather than saline. Our study also had a lower prevalence of lipid core plaque (4% vs. 17% to 48%) because we did not limit analysis to a subset of tissue that was

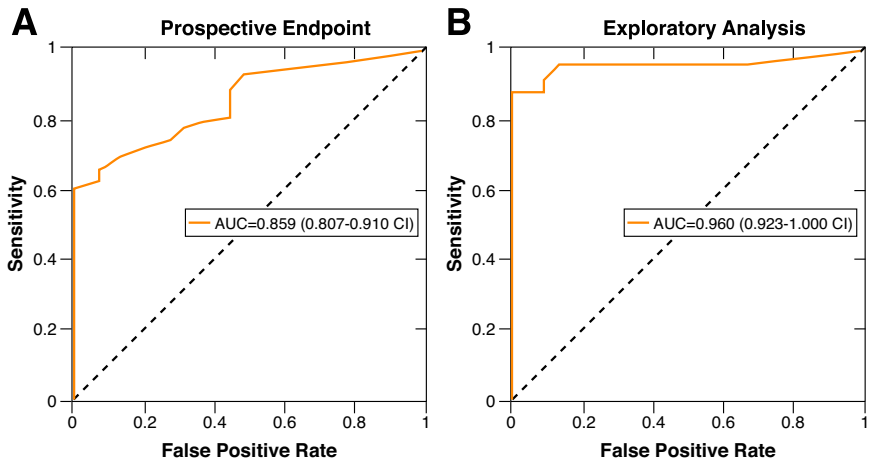

Figure 8. ROC Analysis of Agreement Between LCBI and Histologic Classification

(A) Prospective end point evaluated in all scanned artery segments of adequate quality for detecting presence of lipid core by analysis of NIRS LCBI. **(B)** Retrospective analysis conducted in extreme scanned artery segments with either 0 or >0.2 mm^3 of lipid core volume per millimeter of artery length. Abbreviations as in Figures 1, 5, and 7.

diseased. The analysis of all tissue types through flowing blood yields accuracy calculations that are clinically relevant.

The clinical importance of this autopsy validation is enhanced by the successful use of this catheter in 99 patients with demographic characteristics similar to those of this autopsy study and the recent clearance of the device by the Food and Drug Administration for commercial sales in the U.S. The cost of the catheter will be equivalent to the cost of a drug-eluting stent, and the cost of the console will be equivalent to that of an intravascular ultrasound (IVUS) console.

Exploratory analyses. Exploratory analyses revealed that a major cause of false positives was the occurrence of a NIRS-positive signal over a lipid core that was too small or covered by a cap too thick to meet criteria for a LCP. Lesions with significant lipid but without lipid cores (intimal xanthoma and pathologic intimal thickening) also sometimes resulted in false-positive readings. Such false positives are less a failure of spectroscopy (i.e., lipid was present and generated a NIRS signal) than a sign of the difficulty produced by categorizing various sizes of lipid core plaques and types of lipid accumulation into a binary histology-based classification scheme.

False-negative readings were most frequently produced by lipid cores with extensive calcification, a finding consistent with the presence of fewer lipids in such cores due to displacement of lipid by calcium. The ability of near-infrared light to penetrate through calcium makes it unlikely that near-infrared signals will be affected by "shadowing" artifacts as markedly as are ultrasound examinations.

To test the ability of the NIRS system to discriminate clearly differentiated histologic reference classes, an analysis was performed comparing extremes (LCP with noncalcified lipid cores versus regions without lipid). The AUC of 0.89 (95% CI: 0.85 to 0.94) supports the excellent ability of NIRS to discriminate tissue types based on chemical composition; it is not a measure of the performance obtainable in vivo because the cardiologist cannot eliminate the intermediate histologic areas from a scanned artery using only NIRS and angiography.

The primary end point compares block chemogram intensity readings with the histologic standard in isolated 2-mm blocks and does not use information from adjacent blocks to enhance accuracy. The accuracy of an interpretation comparing positivity by NIRS in 3 or more adjacent blocks versus blocks with no LCP was 0.87 (95% CI: 0.77 to 0.97). This analysis indicates that the appearance of a long and broad yellow signal in the chemogram is an excellent indicator of the presence of a LCP.

Because lipid core plaque intensities generally increase with the size and concentration of focal cholesterol deposits and with the extent of intimal connective tissue degradation, this NIRS device can be characterized as a lipid core plaque detector that is most sensitive to cholesterol-rich regions containing tissue necrosis. Besides a large lipid core, inflammation is another important

JACC: CARDIOVASCULAR IMAGING, VOL. 1, NO. 5, 2008
SEPTEMBER 2008:638–48

characteristic of plaque vulnerable to rupture (15,16). Although the algorithm was not designed to identify the chemical signature of inflammation, there is a close correlation between lipid cores and inflammation (17). This correlation has resulted in successful identification of inflammation indirectly by NIRS (18). NIRS also provides an indirect index of cap thickness because the lipid core signal is attenuated exponentially by the thickness of the cap. However, in the clinical setting, this relationship between signal strength and cap thickness is confounded by variations in both core size and intervening blood layer thickness. Investigational devices that employ optical coherence tomography (11) or optical frequency domain imaging (19) provide the most accurate method to measure cap thickness in the absence of intervening blood.

Study limitations. The current study did not use living tissue. However, because the specimens were maintained on ice and studied soon after death, the target of the imaging (i.e., bulk lipid-rich chemical signatures that are not dependent on living cells) is not likely to differ significantly from the target in living tissue.

Coronary motion was not simulated. However, the high speed of data acquisition (5 ms/spectrum, 40 spectra/s) guarantees that high-quality spectra can be obtained despite cardiac movement.

Finally, the tortuous anatomy of the coronary vasculature was avoided to enhance coregistration of the entire scanned coronary segment with histology. Separate bench testing of the catheter's performance in a tortuous path has verified that the catheter is safe and tracks well in a simulated coronary anatomy.

All 3 of these limitations are due to differences between this ex vivo validation and the clinical application of the device. Ex vivo validation versus histopathology is recommended by the Food and Drug Administration for diagnostic coronary catheters that measure plaque characteristics (20). To experimentally address the limitations of ex vivo validation, the SPECTACL (SPECTroscopic Assessment of Coronary Lipid) clinical study was designed with a primary end point of spectral similarity between in vivo and ex vivo pullbacks, and the end point was achieved (21).

Potential clinical utility of the NIRS system. This successful autopsy validation, together with the clinical results (21) and Food and Drug Administration's 510(k) clearance, indicates that a new, easily used tool to identify lipid core plaques is now available. Lipid core plaque identification will supplement the information about stenosis obtained over the past 40 years with the use of coronary angiography and will open many possibilities for improved risk stratification and treatment that can be tested in formal studies.

For risk stratification, NIRS will facilitate prospective studies testing the hypothesis that the presence of lipid core plaque identifies individual plaques and/or patients at higher risk of a subsequent coronary event. These trials will assist cardiologists in identifying the proper use of this novel technology.

For treatment, knowledge of the presence of lipid core plaques in an artery is likely to be useful in selecting among the 3 major treatments for coronary artery disease—medical therapy, stenting, and bypass surgery—and as a means of improving outcomes within each of the 3 categories.

With regard to medical therapy, identification of extensive lipid core plaque might indicate the need for more aggressive low-density lipoprotein lowering, high-density lipoprotein raising, and antithrombotic therapy.

For stenting therapy, lipid core plaque identification might assist the interventionalist in selecting the optimal length of artery to stent. At present the length to be stented is chosen on the basis of stenosis length as assessed by angiography or IVUS and does not take into account the length of associated lipid core plaque. NIRS may also be helpful for selecting a drug-eluting or bare-metal stent because the endothelium does not grow over drug-eluting stents as well as bare metal stents when located over a lipid core plaque (22).

NIRS has the potential to contribute to resolution of the controversy concerning selection of stenting or medical therapy in patients with stable angina. As reported by Boden et al. (23), a strategy of initial medical care or initial stenting produced similar long-term outcomes for treatment of lesions assessed only on the basis of stenosis. A subsequent trial could be conducted to determine if lipid core lesions respond differently than fibrotic lesions to medical or stenting therapy.

NIRS may also move interventional cardiology closer to toward its goal of prevention of second coronary events from nonstenotic lesions that are "beneath the angiographic radar screen" (24) and would not currently receive local treatment. These lesions are more likely to occur in patients with an acute coronary syndrome in which multiple plaque instability has been documented (25–27).

The combination of NIRS findings with other intravascular measurements should improve diagnostic information. For example, Fukumoto et al. (28) have shown that localized elevation of shear stress, which can be derived from IVUS and flow measurements, is associated with sites of plaque rupture. It is possible that the occurrence of increased shear stress over a LCP increases the risk of rupture and a clinical event. This would explain the well-documented triggering of infarction by heavy exertion, and the association between hemodynamic stress and plaque vulnerability (29,30).

NIRS may also be useful for development of novel antiatherosclerotic drugs as a means to measure changes in composition of a plaque with therapy and to identify very-high risk patients for studies with clinical outcomes.

CONCLUSIONS

A catheter-based NIRS system now available for use in patients has been validated in human coronary autopsy specimens and a clinical trial. This device permits identification of lipid core coronary plaques in patients, thereby supplementing the structural information provided by the coronary angiogram and IVUS. It is expected that this novel capability will lead to multiple studies designed to improve both risk stratification and treatment of patients with coronary artery disease.

Acknowledgments

The authors gratefully acknowledge the individuals whose consent for autopsy studies made this study possible. The authors thank the National Disease Research Interchange and the International Institute for the Advancement of Medicine for supplying the donor hearts, Heddi Avallone at CVPath Institute for the histology slides, Anna Lindquist for morphometric analysis, and Diane Forti for editorial assistance.

Reprint requests and correspondence: Dr. Craig M. Gardner, InfraReDx, Inc., 34 Third Avenue, Burlington, Massachusetts 01803. *E-mail: cgardner@infraredx.com.*

REFERENCES

1. Kolodgie FD, Burke AP, Farb A, , et al. The thin-cap fibroatheroma: a type of vulnerable plaque: the major precursor lesion to acute coronary syndromes. Curr Opin Cardiol 2001;16:285–92.
2. Falk E, Shah PK, Fuster V. Coronary plaque disruption. Circulation 1995;92:657–71.
3. Caplan JD, Waxman S, Nesto RW, Muller JE. Near-infrared spectroscopy for the detection of vulnerable coronary artery plaques. J Am Coll Cardiol 2006;47:C92–6.
4. Waxman S, Ishibashi F, Caplan JD. Rationale and use of near-infrared spectroscopy for detection of lipid-rich and vulnerable plaques. J Nucl Cardiol 2007;14:719–28.
5. Virmani R, Kolodgie FD, Burke AP, Farb A, Schwartz SM. Lessons from sudden coronary death: a comprehensive morphological classification scheme for atherosclerotic lesions. Arterioscler Thromb Vasc Biol 2000;20:1262–75.
6. Hanley JA, McNeil BJ. The meaning and use of the area under a receiver operating characteristic (ROC) curve. Radiology 1982;143:29–36.
7. Rutter CM. Bootstrap estimation of diagnostic accuracy with patient-clustered data. Acad Radiol 2000;7:413–9.
8. Chamuleau SAJ, Meuwissen M, van Eck-Smit BLF, et al. Fractional flow reserve, absolute and relative coronary blood flow velocity reserve in relation to the results of technetium-99m sestambi single-photon emission computed tomography in patients with two-vessel coronary artery disease. J Am Coll Cardiol 2001;37:1316–22.
9. Kawaguchi R, Oshima S, Jingu M, et al. Usefulness of virtual histology intravascular ultrasound to predict distal embolization for ST-segment elevation myocardial infarction. J Am Coll Cardiol 2007;50:1641–6.
10. Zhou X, Obuchowski N, McClish D. Statistical Methods in Diagnostic Medicine. Hoboken, NJ: Wiley, 2002.
11. Yabushita H, Bouma BE, Houser SL, et al. Characterization of human atherosclerosis by optical coherence tomography. Circulation 2002;106:1640–5.
12. Schneiderman J, Wilensky RL, Weiss A, et al. Diagnosis of thin-cap fibroatheromas by a self-contained intravascular magnetic resonance imaging probe in ex vivo human aortas and in situ coronary arteries. J Am Coll Cardiol 2005;45:1961–9.
13. Nair A, Kuban BD, Tuzcu EM, Schoenhagen P, Nissen SE, Vince DG. Coronary plaque classification with intravascular ultrasound radiofrequency data analysis. Circulation 2002;106:2200–6.
14. Schaar JA, De Korte CL, Mastik F, et al. Characterizing vulnerable plaque features with intravascular elastography. Circulation 2003;108:2636–41.
15. Libby P, Ridker PM, Maseri A. Inflammation and atherosclerosis. Circulation 2002;105:1135–43.
16. Hansson GK. Inflammation, atherosclerosis, and coronary artery disease. N Engl J Med 2005;352:1685–95.
17. Rao DS, Goldin JG, Fishbein MC. Determinants of plaque instability in atherosclerotic vascular disease. Cardiovasc Pathol 2005;14:285–93.
18. Moreno PR, Lodder RA, Purushothaman KR, Charash WE, O'Connor WN, Muller JE. Detection of lipid pool, thin fibrous cap, and inflammatory cells in human aortic atherosclerotic plaques by near-infrared spectroscopy. Circulation 2002;105:923–7.
19. Yun SH, Tearney GJ, Vakoc BJ, et al. Comprehensive volumetric optical microscopy in vivo. Nat Med 2006;12:1429–33.
20. Center for Devices and Radiological Health. Guidance for industry and FDA staff: Coronary and peripheral arterial diagnostic catheters. FDA guidance document 1228 [pdf]. Available at: http://www.fda.gov/cdrh/ode/guidance/1228.pdf. Accessed February 18, 2008.

21. Waxman S, L'Allier P, Goldstein J, et al. Detection of lipid rich plaque by near infrared spectroscopy (NIRS) in patients undergoing coronary intervention: results in an unblinded cohort of the SPECTroscopic Assessment of Coronary Lipid (SPECTACL) study (abstr). Am J Cardiol 2007;100 Suppl 1:231L.
22. Oyabu J, Ueda Y, Ogasawara N, Okada K, Hirayama A, Kodama K. Angioscopic evaluation of neointima coverage: sirolimus drug-eluting stent versus bare metal stent. Am Heart J 2006;152:1168–74.
23. Boden WE, O'Rourke RA, Teo KK, et al. Optimal medical therapy with or without PCI for stable coronary disease. N Engl J Med 2007;356:1503–16.
24. Goldstein JA. Angiographic plaque complexity: the tip of the unstable plaque iceberg. J Am Coll Cardiol 2002;39:1464–7.
25. Goldstein JA, Demetriou D, Grines CL, Pica M, Shoukfeh M, O'Neill WW. Multiple complex coronary plaques in patients with acute myocardial infarction. N Engl J Med 2000; 343:915–22.
26. Rioufol G, Finet G, Ginon I, et al. Multiple atherosclerotic plaque rupture in acute coronary syndrome: a three-vessel intravascular ultrasound study. Circulation 2002;106:804–8.
27. Asakura M, Ueda Y, Yamaguchi O, et al. Extensive development of vulnerable plaques as a pan-coronary process in patients with myocardial infarction: an angioscopic study. J Am Coll Cardiol 2001;37:1284–8.
28. Fukumoto Y, Hiro T, Fujii T, et al. Localized elevation of shear stress is related to coronary plaque rupture: a 3-dimensional intravascular ultrasound study with in-vivo color mapping of shear stress distribution. J Am Coll Cardiol 2008;51:645–50.
29. Mittleman MA, Maclure M, Tofler GH, Sherwood JB, Goldberg RJ, Muller JE, on behalf of Myocardial Infarction Onset Study Investigators. Triggering of acute myocardial infarction by heavy physical exertion. Protection against triggering by regular exertion. Determinants of Myocardial Infarction Onset Study Investigators. N Engl J Med 1993;329:1677–83.
30. Muller JE, Abela GS, Nesto RW, Tofler GH. Triggers, acute risk factors and vulnerable plaques: the lexicon of a new frontier. J Am Coll Cardiol 1994;23:809–13.

Key Words: coronary artery disease ■ intravascular imaging ■ near-infrared spectroscopy ■ histopathology ■ ex vivo validation.